yeast Pol II are homologous to RPC1 and RPC2 of Pol III, respectively. Asn620_Lys652 in RPC2 corresponds to Tyr679_Lys712 in RPB2. The deletion of Asn620_Lys652 (Tyr679_Lys712) would destroy a structural core of RPB2, leading to loss of RPB2 function. In addition, Arg768 (Arg852 in RPB2) interacts with the main-chain carbonyl group of Arg70 of the RPB12 subunit, and Asp926 (Asp1009 in RPB2) interacts with the side chain of Arg48 of the RPB10 subunit of Pol II (Figure 1D). Arg768His (Arg852His) and Asp926Glu (Asp1009Glu) substitutions are considered to disturb these subunit interactions, leading to dysfunction of the polymerase. Therefore, structural prediction suggests that the mutations in *POLR3B* (RPC2) could affect Pol III function. On the other hand, Ile897 and Arg1005 in RPC1 correspond to Val863 and Arg1036 in RPB1, respectively. Ile897 (Val863) has hydrophobic interactions with Leu170 and Pro176 of the RPB5 subunit and with Phe900 (Phe866) of the RPB1 subunit of Pol II (Figure 1E). Ile897Asn (Val863Asn) substitution is likely to disturb this interaction. Arg1005 (Arg1036) stabilizes interaction between RPB1 and RPB8 subunits (Figure 1F). The Arg1005Cys (Arg1036Cys) substitution appears to make this interaction unstable. Thus mutations in *POLR3A* are also predicted to affect Pol III function.

Clinical features of individuals with *POLR3A* or *POLR3B* mutations are presented in Table 1. MRI revealed high-intensity areas in the white matter in T2-weighted images, cerebellar atrophy, and a hypoplastic corpus callosum in all four individuals (Figure 3). Individuals 1 and 2 showed an extremely similar clinical course. They developed normally during their early infancy, i.e., walking unaided at 15 and 14 months, and uttering a few words at 12 and 13 months, respectively. After the age of 3, individual 1 presented with unstable walking and frequent stumbling and falling down, and individual 2 became poor at exercise. They both had severe myopia (corrected visual acuity of 0.7 and 0.5 at most, respectively). They graduated from elementary, junior high, and high schools with poor records, and the intelligence quotient (IQ) of individual 2 was 52 (WAIS-III). In individual 1, unstable walking was prominent at around 18 years, and he could not ride a bicycle because of ataxia; however, he could drive an automobile. Amenorrhea was noted in individual 2, and was successfully treated by hormone therapy. Individual 1 showed several signs of hypogonadism, including absence of underarm and mustache hair, thin pubic hair (Tanner II), and serum levels of testosterone, follicle stimulating hormone, and luteinizing hormone that were below normal for age 27. Neurological examination of both individuals revealed mild horizontal nystagmus, slowing of smooth-pursuit eye movement, and gaze limitation, especially in vertical gazing, hypotonia, mildly exaggerated deep-tendon reflex (patellar and Achilles tendon reflex) with negative Babinski reflex, and cerebellar signs and symptoms, including ataxic speech, wide-based ataxic gait, dysdiadochokinesis, and dysmetria. Clinical information for individual 3 has been reported previously.[6] Additional findings are as follows: slowing of smooth-pursuit eye movement, gaze limitation in vertical gazing, normal auditory brain responses (ABR), cerebral symptoms with mild spasticity, and intellectual disability (an IQ of 43 according to the WISC-III test), and no myopia but hypermetropic astigmatism. She showed no deterioration besides a mild dysphagia and walks herself to a school for the disabled. Individual 4 developed normally during his

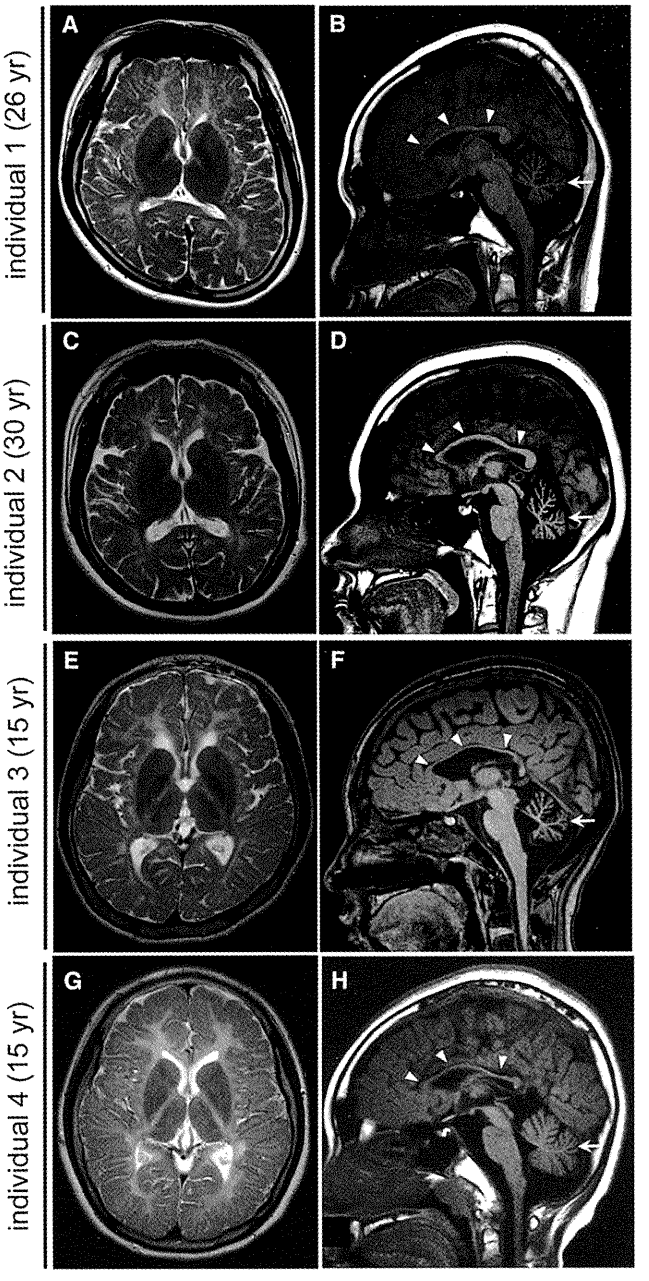

Figure 3. Brain MRI of Individuals with *POLR3B* and *POLR3A* Mutations

(A, C, E, and G) T2-weighted axial images through the basal ganglia. High-intensity areas in the white matter were observed in all individuals.

(B, D, F, and H) T1-weighted midline sagittal images. All the individuals showed hypoplastic corpus callosum (arrowheads) and atrophy of cerebellum (arrows).

early infancy, had normal head control at 3 months, was speaking a few words at 12 months, and was walking unaided at 14 months. His parents noted mild tremors around 4 years. He had normal stature, weight, and head circumference. Although he had severe myopia, his eye movement was smooth with no limitation or nystagmus. He had sensory neuronal deafness on the left side. He showed normal muscle tone and had no spasticity or rigidity. His tendon reflexes were slightly elevated with a negative Babinski reflex. Cerebellar signs were noted; expressive ataxic explosive speech, intension tremor, poor finger to nose test, dysdiadochokinesis, dysmetria, and wide-based ataxic gait. His intelligence quotient was 57 (according to the WISC-III test). His peripheral nerve conduction velocity was within the normal range and his ABR showed normal responses on the right side. He suffered motor deterioration around age 14 and became wheelchair bound.

In this study, we successfully identified compound heterozygous mutations in *POLR3A* and *POLR3B* in individuals with HCAHC. Very recently, Bernard et al.[12] reported that *POLR3A* mutations cause three overlapping leukodystrophies, including 4H syndrome, suggesting that HCAHC is, at least in part, within a wide clinical spectrum caused by *POLR3A* mutations. The p.Arg1005Cys mutation was shared between individual 9 in their report and our individual 4. All 19 individuals with *POLR3A* mutations showed progressive upper motor neuron dysfunction and cognitive regression. In addition, individual 9 showed abnormal eye movement, hypodontia, and hypogonadism. None of these features were recognized in our individual 4; these differences further support phenotypic variability of *POLR3A* mutations.[12] Given the phenotypic similarities among 4H syndrome, HCAHC, and H-ABC, there is a possibility that H-ABC is also allelic and caused by recessive mutations in either *POLR3A* or *POLR3B*.

Pol III consists of 17 subunits and is involved in the transcription of small noncoding RNAs, such as 5S ribosomal RNA (rRNA), U6 small nuclear RNA (snRNA), 7SL RNA, RNase P, RNase MRP, short interspersed nuclear elements (SINEs), and all transfer RNAs (tRNAs). Pol III-transcribed genes are classified into three types based on promoter elements and transcription factors. 5S rRNA is a solo type I gene. Type II genes include tRNA, 7SL RNA, and SINEs. Type III genes include U6 snRNA, RNase P, and RNase MRP.[18–20] The Pol III system is important for cell growth in yeast, and its transcription is tightly regulated during the cell cycle.[20] In zebrafish, *polr3b* mutant larvae that have a deletion of 41 conserved amino acids (Δ239-279) from the Rpc2 protein showed a proliferation deficit in multiple tissues, including intestine, endocrine pancreas, liver, retina and terminal branchial arches.[21] In the mutants, the expression levels of tRNA were significantly reduced, whereas the level of 5S rRNA expression was not changed, suggesting that this *polr3b* mutation can differentially affect Pol III target promoters.[21] RPC2 contributes to the catalytic activity of the polymerase and forms the active center of the polymerase together with the largest subunit, RPC1.[22] Thus, it is reasonable to consider that mutations in *POLR3A* and *POLR3B* cause overlapping phenotypes. Indeed, three individuals with *POLR3B* mutations showed diffuse cerebral hypomyelination, atrophy of the cerebellum and corpus callosum, and abnormal eye movements that overlap with *POLR3A* abnormalities.[12] Furthermore, two out of three individuals showed hypogonadism, suggesting a common pathological mechanism between *POLR3A* and *POLR3B* mutations. In the zebrafish *polr3b* mutants there were no defects of the central nervous system other than a reduced size of the retina, probably reflecting species differences; however, the reduced level of tRNA in the *polr3b* mutants raises the possibility that defects of tRNA transcription by Pol III could be a common pathological mechanism underlying *POLR3A* and *POLR3B* mutations. Supporting this idea, mutations in two genes involved in aminoacylation activity of tRNA synthetase cause defects of myelination in central nervous system: *DARS2* (MIM 610956) and *AIMP* (MIM 603605).[23,24] In addition, mutations in four genes encoding aminoacyl-tRNA synthetase cause Charcot-Marie-Tooth disease (MIM 613641, 613287, 601472, and 608323), resulting from demyelination of peripheral nerve axons: *KARS* (MIM 601421), *GARS* (MIM 600287), *YARS* (MIM 603623), and *AARS* (MIM 601065).[25–28] Thus, it is very likely that regulation of tRNA expression is essential for development and maintenance of myelination in both central and peripheral nervous systems.

An interesting clinical feature of *POLR3B* mutations is the absence of motor deterioration. All three individuals with *POLR3B* mutations could walk without support at ages 16, 27, and 30, whereas individual 3 with *POLR3A* mutations had motor deterioration around age 14. Bernard et al.[12] also reported progressive upper motor neuron dysfunction and cognitive regression in individuals with *POLR3A* mutations. Thus, there is a possibility that phenotypes caused by *POLR3A* mutations could be more severe and progressive than *POLR3B* mutant phenotypes. Identification of a greater number of cases with *POLR3B* mutations is required to confirm this hypothesis.

In conclusion, our data, together with that of a previous report,[12] demonstrate that mutations in Pol III subunits cause overlapping autosomal-recessive hypomyelinating disorders. Establishment of an animal model will facilitate our understanding of the pathophysiology of the multiple defects caused by Pol III mutations.

Supplemental Data

Supplemental Data include three tables and can be found with this article online at http://www.cell.com/AJHG/.

Acknowledgments

We would like to thank all the individuals and their families for their participation in this study. This work was supported by

research grants from the Ministry of Health, Labour, and Welfare (H.S., H.O., M.S., J.T., N. Miyake, K.I. and N. Matsumoto), the Japan Science and Technology Agency (N. Matsumoto), a Grant-in-Aid for Scientific Research on Innovative Areas (Foundation of Synapse and Neurocircuit Pathology) from the Ministry of Education, Culture, Sports, Science and Technology of Japan (N. Matsumoto), a Grant-in-Aid for Scientific Research from Japan Society for the Promotion of Science (H.O., N. Matsumoto), a Grant-in-Aid for Young Scientist from Japan Society for the Promotion of Science (H.S.). This work has been done at Advanced Medical Research Center, Yokohama City University.

Received: August 31, 2011
Revised: October 5, 2011
Accepted: October 10, 2011
Published online: October 27, 2011

Web Resources

The URLs for data presented herein are as follows:

ClustalW, http://www.genome.jp/tools/clustalw/
dbSNP, http://www.ncbi.nlm.nih.gov/projects/SNP/
Ensembl, http://uswest.ensembl.org/index.html
GenBank, http://www.ncbi.nlm.nih.gov/Genbank/
Online Mendelian Inheritance in Man, http://www.omim.org
PolyPhen-2, http://genetics.bwh.harvard.edu/pph2/
Protein Data Bank, http://www.pdb.org/pdb/home/home.do
PyMOL, http://www.pymol.org/
SeattleSeq Annotation, http://gvs.gs.washington.edu/SeattleSeqAnnotation/

References

1. Schiffmann, R., and van der Knaap, M.S. (2009). Invited article: an MRI-based approach to the diagnosis of white matter disorders. Neurology *72*, 750–759.
2. Timmons, M., Tsokos, M., Asab, M.A., Seminara, S.B., Zirzow, G.C., Kaneski, C.R., Heiss, J.D., van der Knaap, M.S., Vanier, M.T., Schiffmann, R., and Wong, K. (2006). Peripheral and central hypomyelination with hypogonadotropic hypogonadism and hypodontia. Neurology *67*, 2066–2069.
3. Wolf, N.I., Harting, I., Boltshauser, E., Wiegand, G., Koch, M.J., Schmitt-Mechelke, T., Martin, E., Zschocke, J., Uhlenberg, B., Hoffmann, G.F., et al. (2005). Leukoencephalopathy with ataxia, hypodontia, and hypomyelination. Neurology *64*, 1461–1464.
4. Wolf, N.I., Harting, I., Innes, A.M., Patzer, S., Zeitler, P., Schneider, A., Wolff, A., Baier, K., Zschocke, J., Ebinger, F., et al. (2007). Ataxia, delayed dentition and hypomyelination: a novel leukoencephalopathy. Neuropediatrics *38*, 64–70.
5. van der Knaap, M.S., Naidu, S., Pouwels, P.J., Bonavita, S., van Coster, R., Lagae, L., Sperner, J., Surtees, R., Schiffmann, R., and Valk, J. (2002). New syndrome characterized by hypomyelination with atrophy of the basal ganglia and cerebellum. AJNR Am. J. Neuroradiol. *23*, 1466–1474.
6. Sasaki, M., Takanashi, J., Tada, H., Sakuma, H., Furushima, W., and Sato, N. (2009). Diffuse cerebral hypomyelination with cerebellar atrophy and hypoplasia of the corpus callosum. Brain Dev. *31*, 582–587.
7. Li, H., Ruan, J., and Durbin, R. (2008). Mapping short DNA sequencing reads and calling variants using mapping quality scores. Genome Res. *18*, 1851–1858.
8. Doi, H., Yoshida, K., Yasuda, T., Fukuda, M., Fukuda, Y., Morita, H., Ikeda, S., Kato, R., Tsurusaki, Y., Miyake, N., et al. (2011). Exome sequencing reveals a homozygous *SYT14* mutation in adult-onset, autosomal-recessive spinocerebellar ataxia with psychomotor retardation. Am. J. Hum. Genet. *89*, 320–327.
9. Pierce, S.B., Walsh, T., Chisholm, K.M., Lee, M.K., Thornton, A.M., Fiumara, A., Opitz, J.M., Levy-Lahad, E., Klevit, R.E., and King, M.C. (2010). Mutations in the DBP-deficiency protein HSD17B4 cause ovarian dysgenesis, hearing loss, and ataxia of Perrault Syndrome. Am. J. Hum. Genet. *87*, 282–288.
10. Gilissen, C., Arts, H.H., Hoischen, A., Spruijt, L., Mans, D.A., Arts, P., van Lier, B., Steehouwer, M., van Reeuwijk, J., Kant, S.G., et al. (2010). Exome sequencing identifies *WDR35* variants involved in Sensenbrenner syndrome. Am. J. Hum. Genet. *87*, 418–423.
11. Saitsu, H., Kato, M., Okada, I., Orii, K.E., Higuchi, T., Hoshino, H., Kubota, M., Arai, H., Tagawa, T., Kimura, S., et al. (2010). *STXBP1* mutations in early infantile epileptic encephalopathy with suppression-burst pattern. Epilepsia *51*, 2397–2405.
12. Bernard, G., Chouery, E., Putorti, M.L., Tetreault, M., Takanohashi, A., Carosso, G., Clement, I., Boespflug-Tanguy, O., Rodriguez, D., Delague, V., et al. (2011). Mutations of *POLR3A* Encoding a Catalytic Subunit of RNA Polymerase Pol III Cause a Recessive Hypomyelinating Leukodystrophy. Am. J. Hum. Genet. *89*, 415–423.
13. Jasiak, A.J., Armache, K.J., Martens, B., Jansen, R.P., and Cramer, P. (2006). Structural biology of RNA polymerase III: subcomplex C17/25 X-ray structure and 11 subunit enzyme model. Mol. Cell *23*, 71–81.
14. Fernández-Tornero, C., Böttcher, B., Riva, M., Carles, C., Steuerwald, U., Ruigrok, R.W., Sentenac, A., Müller, C.W., and Schoehn, G. (2007). Insights into transcription initiation and termination from the electron microscopy structure of yeast RNA polymerase III. Mol. Cell *25*, 813–823.
15. Cramer, P., Bushnell, D.A., and Kornberg, R.D. (2001). Structural basis of transcription: RNA polymerase II at 2.8 angstrom resolution. Science *292*, 1863–1876.
16. Gnatt, A.L., Cramer, P., Fu, J., Bushnell, D.A., and Kornberg, R.D. (2001). Structural basis of transcription: an RNA polymerase II elongation complex at 3.3 A resolution. Science *292*, 1876–1882.
17. Wang, D., Bushnell, D.A., Huang, X., Westover, K.D., Levitt, M., and Kornberg, R.D. (2009). Structural basis of transcription: backtracked RNA polymerase II at 3.4 angstrom resolution. Science *324*, 1203–1206.
18. Oler, A.J., Alla, R.K., Roberts, D.N., Wong, A., Hollenhorst, P.C., Chandler, K.J., Cassiday, P.A., Nelson, C.A., Hagedorn, C.H., Graves, B.J., and Cairns, B.R. (2010). Human RNA polymerase III transcriptomes and relationships to Pol II promoter chromatin and enhancer-binding factors. Nat. Struct. Mol. Biol. *17*, 620–628.
19. Dieci, G., Fiorino, G., Castelnuovo, M., Teichmann, M., and Pagano, A. (2007). The expanding RNA polymerase III transcriptome. Trends Genet. *23*, 614–622.
20. Dumay-Odelot, H., Durrieu-Gaillard, S., Da Silva, D., Roeder, R.G., and Teichmann, M. (2010). Cell growth- and differentiation-dependent regulation of RNA polymerase III transcription. Cell Cycle *9*, 3687–3699.

21. Yee, N.S., Gong, W., Huang, Y., Lorent, K., Dolan, A.C., Maraia, R.J., and Pack, M. (2007). Mutation of RNA Pol III subunit *rpc2/polr3b* Leads to Deficiency of Subunit Rpc11 and disrupts zebrafish digestive development. PLoS Biol. *5*, e312.
22. Werner, M., Thuriaux, P., and Soutourina, J. (2009). Structure-function analysis of RNA polymerases I and III. Curr. Opin. Struct. Biol. *19*, 740–745.
23. Scheper, G.C., van der Klok, T., van Andel, R.J., van Berkel, C.G., Sissler, M., Smet, J., Muravina, T.I., Serkov, S.V., Uziel, G., Bugiani, M., et al. (2007). Mitochondrial aspartyl-tRNA synthetase deficiency causes leukoencephalopathy with brain stem and spinal cord involvement and lactate elevation. Nat. Genet. *39*, 534–539.
24. Feinstein, M., Markus, B., Noyman, I., Shalev, H., Flusser, H., Shelef, I., Liani-Leibson, K., Shorer, Z., Cohen, I., Khateeb, S., et al. (2010). Pelizaeus-Merzbacher-like disease caused by AIMP1/p43 homozygous mutation. Am. J. Hum. Genet. *87*, 820–828.
25. Latour, P., Thauvin-Robinet, C., Baudelet-Méry, C., Soichot, P., Cusin, V., Faivre, L., Locatelli, M.C., Mayençon, M., Sarcey, A., Broussolle, E., et al. (2010). A major determinant for binding and aminoacylation of tRNA(Ala) in cytoplasmic Alanyl-tRNA synthetase is mutated in dominant axonal Charcot-Marie-Tooth disease. Am. J. Hum. Genet. *86*, 77–82.
26. McLaughlin, H.M., Sakaguchi, R., Liu, C., Igarashi, T., Pehlivan, D., Chu, K., Iyer, R., Cruz, P., Cherukuri, P.F., Hansen, N.F., et al. (2010). Compound heterozygosity for loss-of-function lysyl-tRNA synthetase mutations in a patient with peripheral neuropathy. Am. J. Hum. Genet. *87*, 560–566.
27. Antonellis, A., Ellsworth, R.E., Sambuughin, N., Puls, I., Abel, A., Lee-Lin, S.Q., Jordanova, A., Kremensky, I., Christodoulou, K., Middleton, L.T., et al. (2003). Glycyl tRNA synthetase mutations in Charcot-Marie-Tooth disease type 2D and distal spinal muscular atrophy type V. Am. J. Hum. Genet. *72*, 1293–1299.
28. Jordanova, A., Irobi, J., Thomas, F.P., Van Dijck, P., Meerschaert, K., Dewil, M., Dierick, I., Jacobs, A., De Vriendt, E., Guergueltcheva, V., et al. (2006). Disrupted function and axonal distribution of mutant tyrosyl-tRNA synthetase in dominant intermediate Charcot-Marie-Tooth neuropathy. Nat. Genet. *38*, 197–202.

A novel adult case of juvenile-onset Alexander disease: complete remission of neurological symptoms for over 12 years, despite insidiously progressive cervicomedullary atrophy

Michito Namekawa, Yoshihisa Takiyama, Junko Honda, Kumi Sakoe, Tametou Naoi, Haruo Shimazaki, Takanori Yamagata, Mariko Y. Momoi,

Neurological Sciences
Official Journal of the Italian Neurological Society

ISSN 1590-1874

Neurol Sci
DOI 10.1007/s10072-011-0902-z

Springer

Springer

Neurol Sci
DOI 10.1007/s10072-011-0902-z

CASE REPORT

A novel adult case of juvenile-onset Alexander disease: complete remission of neurological symptoms for over 12 years, despite insidiously progressive cervicomedullary atrophy

Michito Namekawa · Yoshihisa Takiyama · Junko Honda · Kumi Sakoe · Tametou Naoi · Haruo Shimazaki · Takanori Yamagata · Mariko Y. Momoi · Imaharu Nakano

Received: 24 December 2010 / Accepted: 14 December 2011

Abstract We present here a 25-year-old woman with genetically confirmed (p.R276L mutation in the *GFAP* gene) juvenile-onset AxD. Episodic vomiting appeared at age nine, causing anorexia and insufficient growth. Brain MRI at age 11 showed a small nodular lesion with contrast enhancement in the left dorsal portion of the cervicomedullary junction. Her episodic vomiting improved spontaneously at age 13, and she became neurologically asymptomatic. The enhancement of the lesion disappeared simultaneously, although the plaque remained. Longitudinal MRI observations, however, revealed insidiously progressive cervicomedullary atrophy without a signal change. This case broadens our knowledge of AxD: (1) molecular analysis of the *GFAP* gene is warranted in patients with MRI evidence of tumor-like lesions in the brainstem, particularly if they present with isolated episodic vomiting and/or anorexia; (2) the disease can be self-remitting for at least 12 years; (3) cervicomedullary atrophy, characteristic of the adult form, can be insidiously progressive without a signal change before the clinical symptoms appear.

M. Namekawa (✉) · J. Honda · K. Sakoe · T. Naoi · H. Shimazaki · I. Nakano
Department of Neurology, Jichi Medical University, 3311-1, Yakushiji, Shimotsuke, Tochigi 329-0498, Japan
e-mail: mnamekaw@jichi.ac.jp

Y. Takiyama
Department of Neurology, Interdisciplinary Graduate School of Medicine and Engineering, University of Yamanashi, Kofu, Japan

T. Yamagata · M. Y. Momoi
Department of Pediatrics, Jichi Medical University, Shimotsuke, Japan

Published online: 24 December 2011

Keywords Alexander disease · GFAP · Vomiting · Anorexia nervosa · Remission · Cervicomedullary atrophy

Introduction

Typical Alexander disease (AxD) (OMIM #203450) is a lethal infantile leukoencephalopathy with frontal predominance characterized by Rosenthal fiber deposition in astrocytes (reviewed in [1]). The discovery that mutations in the gene coding glial fibrillary acidic protein (GFAP) are responsible for AxD has led to the identification of both juvenile (age at onset: 2–12 years) and adult (age at onset: over 12 years) forms of the disease. Each subtype is characterized by specific MRI findings: in the juvenile form, tumor-like nodular and/or swollen lesions in the brainstem [2, 3]; in the adult form, a distinctive tadpole-like brainstem atrophy, consisting of severe atrophy of the medulla oblongata and cervical spinal cord, with an intact pontine base [4, 5]. The reason for the age-related variability of the lesions in AxD remains unclear.

We present here a novel case of genetically confirmed AxD. The patient's episodic vomiting improved spontaneously and she became neurologically asymptomatic, although longitudinal observations for more than 12 years revealed insidiously progressive cervicomedullary atrophy.

Case report

The patient, a 25-year-old Japanese woman, the second child of non-consanguineous healthy parents, was born after 39 weeks of gestation with no prenatal or perinatal problems. Her early developmental milestones were normal, except for two episodes of febrile seizures at 1 year of

age, which never recurred. From the age of three, her food intake was relatively small, and malnutrition delayed her physical growth, but her mental development was normal. From the age of nine, she suffered from episodic vomiting after eating, which caused anorexia. At the age of 11, she was referred to our hospital for further investigation of progressive weight loss (−1.4 kg/year). Her height was 123 cm (−3.0 SD) and she weighed 18.6 kg (−2.5 SD). She had normal intelligence and no neurological deficits, except for episodic postprandial vomiting. Detailed physical investigations showed no significant abnormalities, except for scoliosis. Gastrointestinal, metabolic, endocrinological and psychological disorders were ruled out. No neurophysiological examinations were performed, although, brain MRI revealed a 7-mm-sized lesion in the posterior dorsal portion of the cervicomedullary junction, which was enhanced with Gd-DTPA (Fig. 1A). Signal changes were also detected bilaterally in the dentate nuclei without enhancement. No other signal abnormalities were noted. During follow-up on MRIs, taken twice a year, the enhancement of the lesion disappeared after 2 years, although the plaque remained. Her episodic vomiting also vanished almost simultaneously. Her growth stopped at the age of 17. At age 25, she is frail 140 cm/33.4 kg with scoliosis. She has normal intelligence and is asymptomatic. A tiny plaque without enhancement, the same size as before, is still visible in the dorsal part of medulla oblongata (Fig. 1C), although cervicomedullary atrophy without a signal change has advanced (Fig. 1B).

Sequencing of the *GFAP* gene with informed consent revealed a heterozygous missense mutation in exon 5 (c.827G>T), causing a change of arginine to leucine at amino acid position 276 (p.R276L). The mutation was not found in her mother. The father, who died in traffic accident in his forties, could not be investigated. This mutation has already been described as responsible for pathologically proven hereditary [4] and sporadic [5] cases of adult-onset AxD. According to an interview, there was no relationship between the present patient and the families previously reported, although they originated from the same region of Japan.

Discussion

We present a Japanese patient with genetically confirmed juvenile-onset AxD. Episodic vomiting, which was the only sign of bulbar dysfunction, caused malnutrition and weight loss, probably related to a tiny lesion seen by MRI in dorsal part of medulla oblongata, presumably involving the "area postrema", which plays an essential role in the system controlling feeding [6]. Similar cases have already been reported [7, 8], but the patients in the literature also had additional bulbar symptoms, such as dysphagia and dysphonia. This case indicates that a molecular analysis of the *GFAP* gene is warranted in patients with MRI evidence of even tiny tumor-like lesions in the brainstem, particularly if they present with isolated episodic vomiting and/or anorexia.

It is noteworthy that the bulbar symptom of this patient regressed spontaneously. She is now 25 years old, and is absolutely free of neurological symptoms, except for short stature with scoliosis, presumably a sign of AxD [9]. This case suggests that the symptoms of AxD can be self-remitting, unlike those of other neurodegenerative disorders, and that the prognosis might not necessarily be unfavorable. To our knowledge, no other AxD patient whose symptoms vanished for such a long period of time has been reported in the literature. Very recently, a case of adult-onset AxD with remission and relapse was reported, but the remission was only partial and lasted less than 5 years [10]; atypical AxD has been mistaken for remitting–relapsing multiple sclerosis [1]. Because the cervicomedullary atrophy continues to progress in our patient (Fig. 1B), she might still develop an adult form of the disease in the future.

The longitudinal observation of progressive cervicomedullary atrophy, which is characteristic of the adult AxD [4, 5], is interesting. It has been speculated that brainstem atrophy in the adult form of AxD might result from tissue damage related to the contrast enhanced nodular and/or swollen lesions usually observed in the juvenile form of the disease. A recent report of a patient with progressive medullary atrophy has reinforced this hypothesis [11]. The 20-year-old patient had an expanded cervicomedullary lesion with patchy contrast enhancement; progressive atrophy was observed 5.5 years later [11].

Our case differs, however, in that the medullary lesion was confined to a tiny portion of the dorsal region, and seems too small to be responsible for expansion of the cervicomedullary lesion, suggesting that the latter, which is reminiscent of chronic progressive neuro-Behçet's disease, results from a different pathological process. [12]. In neuro-Behçet's disease, subacute brainstem encephalitis, which is the most common in parenchymal involvement, shows hypertense T2 lesion with contrast enhancement. Spontaneous self-remission without therapy has been reported, although, some patients develop a slowly progressive disease with insidiously advancing brainstem atrophy [12].

Observation of our patient for over 14 years, allowed us to demonstrate, for the first time, that the marked cervicomedullary atrophy characteristic of adult-onset AxD might result from an insidiously progressive process. More patients will be needed to determine whether a nodular lesion with contrast enhancement, however small, is

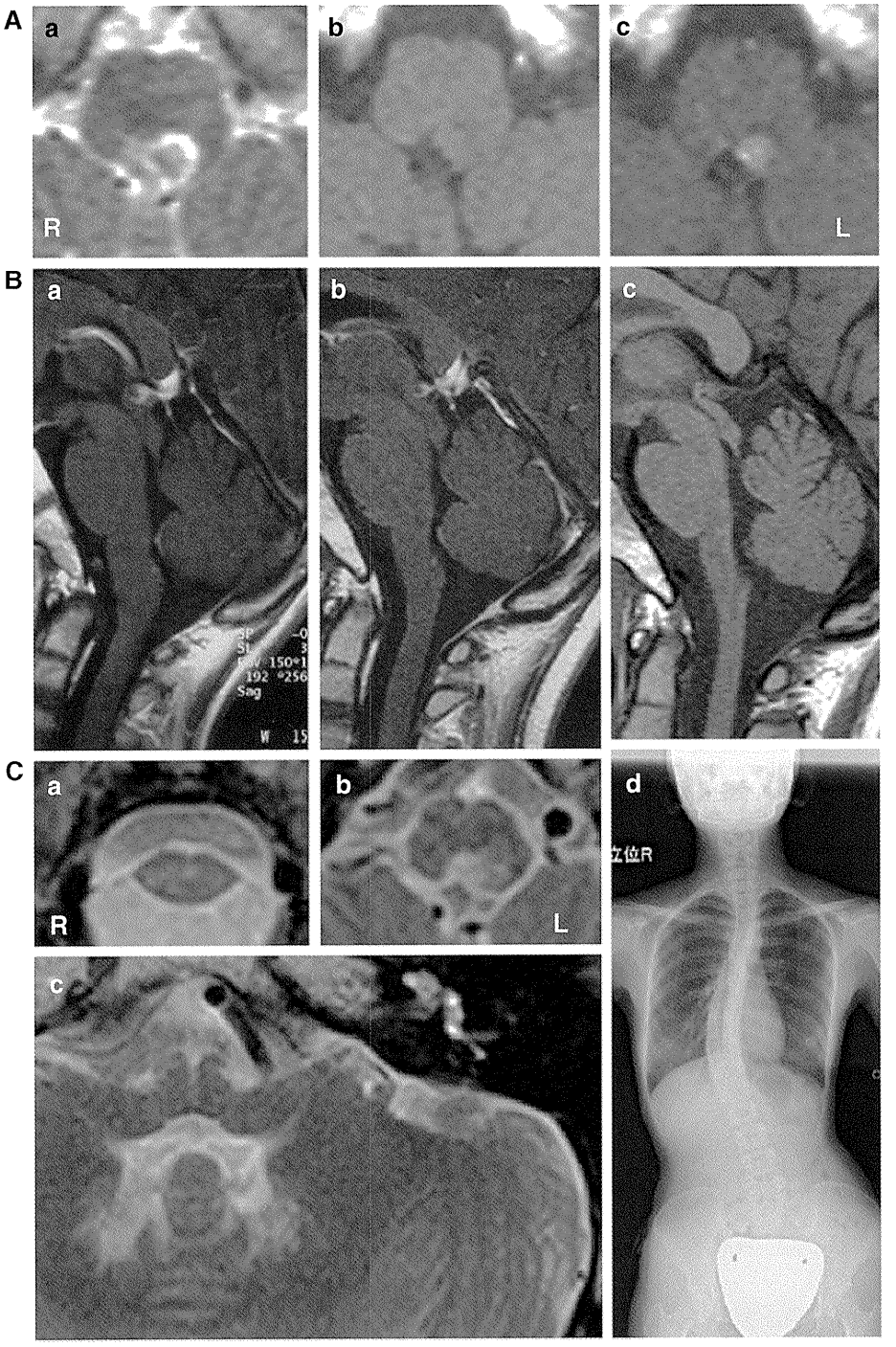

Fig. 1 Serial radiological studies. **A** First MRI of the medulla oblongata (at age 11): axial T2-weighted image (T2-WI) (*a*), T1-WI (*b*), and T1-WI with gadolinium enhancement (*c*) of axial sections. The lesion is 7 mm in size, hyper-intense, but hypo-intense inside on T2-WI (*a*), iso- to hypo-intense on T1-WI (*b*), with contrast enhancement (*c*). Except for the bilateral hilus of the dentate nucleus (same as 14 years later; **C**-*c*), no other signal abnormalities were noted (data not shown). The enhancement disappeared 2 years later (data not shown), although, the plaque remains. **B** Chronological sagittal section of the brainstem MRI at age 11 (*a*), 16 (*b*) and 25 (*c*). Brainstem atrophy is unremarkable at age 11 (*a*), although, with time, progressive atrophy of medulla oblongata is seen (*b*, *c*). The anterior–posterior diameter at the middle of the medulla oblongata was 11.7 mm at age 11 (*a*), but only 8.8 mm at age 25 (*c*). **C** Radiological study at age 25. Axial T2-WI (*a*–*c*). Moderate atrophy of cervical spinal cord (*a*) and medulla (*b*) are seen. A small plaque in the dorsal part of medulla oblongata (*b*) without contrast enhancement (data not shown) remains, although its size has not changed since age 11 (**A**-*a*). The hilus of the dentate nucleus is hyper-intense bilaterally without enhancement (data not shown), although, no other signal change is detected in the brainstem (*c*). No pontine or midbrain atrophy, abnormalities in the basal ganglia, "ventricular garlands" or leuko-dystrophy in deep white matter were observed (data not shown). Mild scoliosis was also observed in this patient (*d*)

essential to trigger the cervicomedullary atrophy or whether the mutation in the *GFAP* gene is sufficient.

Acknowledgments This work was supported by Alexander disease research grants from the Intractable Disease Research Grants, from the Ministry of Health, Labour and Welfare of the government of Japan. We are very grateful to Dr. Merle Ruberg for critical reading of this manuscript.

References

1. Brenner M, Goldman JE, Quinlan RA, Messing A (2009) Alexander disease: a genetic disorder of astrocytes, chap 24. In: Parpura V, Haydon PG (eds) Astrocytes in (patho)physiology of the nervous system. Springer, New York, pp 591–647
2. van der Knaap MS, Salomons GS, Li R, Franzoni E, Gutiérrez-Solana LG, Smit LME, Robinson R, Ferrie CD, Cree B, Reddy A, Thomas N, Banwell B, Barkhof F, Jakobs C, Johnson A, Messing A, Brenner M (2005) Unusual variants of Alexander's disease. Ann Neurol 57:327–338. doi:10.1002/ana.20381
3. van der Knaap MS, Ramesh V, Schiffmann R, Blaser S, Kyllerman M, Gholkar A, Ellison DW, van der Voorn JP, van Dooren SJM, Jakobs C, Barkhof F, Salomons GS (2006) Alexander disease. Ventricular garlands and abnormalities of the medulla and spinal cord. Neurology 66:494–498. doi:10.1212/01.wnl.0000198770.80743.37
4. Namekawa M, Takiyama Y, Aoki Y, Takayashiki N, Sakoe K, Shimazaki H, Taguchi T, Tanaka Y, Nishizawa M, Saito K, Matsubara Y, Nakano I (2002) Identification of *GFAP* gene mutation in hereditary adult-onset Alexander's disease. Ann Neurol 52:779–785. doi:10.1002/ana.10375
5. Namekawa M, Takiyama Y, Honda J, Shimazaki H, Sakoe K, Nakano I (2010) Adult-onset Alexander disease with typical "tadpole" brainstem atrophy and unusual bilateral basal ganglia involvement: a case report and review of the literature. BMC Neurology10:21. doi:10.1186/1471-2377-10-21
6. Price CJ, Hoyda TD, Ferguson AV (2008) The area postrema: a brain monitor and integrator of systemic autonomic state. Neuroscientist 14:182–194. doi:10.1177/1073858407311100
7. Franzoni E, van der Knaap MS, Errani A, Colonnelli MC, Bracceschi R, Malaspina E, Moscano FC, Garone C, Sarajlija J, Zimmerman RA, Salomons GS, Bernardi B (2006) Unusual diagnosis in a child suffering from juvenile Alexander disease: clinical and imaging report. J Child Neurol 21:1075–1080. doi:10.1177/7010.2006.00235
8. Niinikoski H, Haataja L, Brander A, Valanne L, Blaser S (2009) Alexander disease as a cause of nocturnal vomiting in a 7-year-old girl. Pediatr Radiol 39:872–875. doi:10.1007/s00247-009-1289-3
9. Ozturk C, Tezer M, Karatoprak O, Hamzaoglu A (2009) A rare cause of neuromuscular scoliosis: Alexander disease. Joint Bone Spine 76:195–197. doi:10.1016/j.jbspin.2008.06.012
10. Ayaki T, Shinohara M, Tatsumi S, Namekawa M, Yamamoto T (2010) A case of sporadic adult Alexander disease presenting with acute onset, remission and relapse. J Neurol Neurosurg Psychiatry 81:1292–1293. doi:10.1136/jnnp.2009.178079
11. Romano S, Salvetti M, Ceccherini I, De Simone T, Savoiardo M (2007) Brainstem signs with progressing atrophy of medulla oblongata and upper cervical spinal cord. Lancet Neurol 6:562–570. doi:10.1016/S1474-4422(07)70129-1
12. Al-Araji A, Kidd DP (2009) Neuro-Behçet's disease: epidemiology, clinical characteristics, and management. Lancet Neurol 8:192–204. doi:10.1016/S1474-4422(09)70015-8

ELSEVIER

Brain & Development 32 (2010) 171–179

BRAIN & DEVELOPMENT
Official Journal of the Japanese Society of Child Neurology

www.elsevier.com/locate/braindev

Original article

Comprehensive genetic analyses of *PLP1* in patients with Pelizaeus–Merzbacher disease applied by array-CGH and fiber-FISH analyses identified new mutations and variable sizes of duplications

Keiko Shimojima [a], Takehiko Inoue [b], Ai Hoshino [c,d], Satsuki Kakiuchi [e], Yoshiaki Watanabe [f], Masayuki Sasaki [g], Akira Nishimura [g], Akiko Takeshita-Yanagisawa [h], Go Tajima [i], Hiroshi Ozawa [c,j], Masaya Kubota [c,k], Jun Tohyama [l], Masayuki Sasaki [m], Akira Oka [k,n], Kayoko Saito [o], Makiko Osawa [h], Toshiyuki Yamamoto [a,*]

[a] *International Research and Educational Institute for Integrated Medical Sciences (IREIIMS), Tokyo Women's Medical University, 8-1 Kawada-cho, Shinjuku-ward, Tokyo 162-8666, Japan*
[b] *Division of Child Neurology, Institute of Neurological Sciences, Faculty of Medicine, Tottori University, Yonago, Japan*
[c] *Department of Pediatrics, Tokyo Metropolitan Hachioji Children's Hospital, Hachioji, Japan*
[d] *Department of Neuropediatrics, Tokyo Metropolitan Neurological Hospital, Fuchu, Japan*
[e] *Department of Neonatology, Tokyo Metropolitan Bokutoh Hospital, Tokyo, Japan*
[f] *Department of Child Neurology, Okayama University Graduate School of Medicine, Okayama, Japan*
[g] *Department of Pediatrics, Kyoto Prefectural University of Medicine, Kyoto, Japan*
[h] *Department of Pediatrics, Faculty of Medicine, Tokyo Women's medical University, Tokyo, Japan*
[i] *Department of Pediatrics, Hiroshima University Graduate School of Biomedical Sciences, Hiroshima, Japan*
[j] *Shimada Ryoiku Center, Tama, Japan*
[k] *Division of Child Neurology, National Center of Child Health and Development, Tokyo, Japan*
[l] *Epilepsy Center, National Nishi-Niigata Chuo National Hospital, Niigata, Japan*
[m] *Department of Child Neurology, National Center Hospital for Mental, Nervous and Muscular Disorders, National Center of Neurology and Psychiatry, Kodaira, Japan*
[n] *Department of Pediatrics, Faculty of Medicine, The University of Tokyo, Tokyo, Japan*
[o] *Institute of Medical Genetics, Tokyo Women's medical University, Tokyo, Japan*

Received 22 November 2008; received in revised form 2 February 2009; accepted 22 February 2009

Abstract

Pelizaeus–Merzbacher disease (PMD; MIM#312080) is a rare X-linked recessive neurodegenerative disorder. The main cause of PMD is alterations in the proteolipid protein 1 gene (*PLP1*) on chromosome Xq22.2. Duplications and point mutations of *PLP1* have been found in 70% and 10–25% of all patients with PMD, respectively, with a wide clinical spectrum. Since the underlining genomic abnormalities are heterogeneous in patients with PMD, clarification of the genotype-phenotype correlation is the object of this study. Comprehensive genetic analyses using microarray-based comparative genomic hybridization (aCGH) analysis and genomic sequencing were applied to fifteen unrelated male patients with a clinical diagnosis of PMD. Duplicated regions were further analyzed by fiber-fluorescence *in situ* hybridization (FISH) analysis. Four novel and one known nucleotide alterations were identified in five patients. Five microduplications including *PLP1* were identified by aCGH analysis with the sizes ranging from

* Corresponding author. Tel.: +81 3 3353 8111; fax: +81 3 3352 3088
E-mail address: yamamoto@imcir.twmu.ac.jp (T. Yamamoto).

0387-7604/$ - see front matter
doi:10.1016/j.braindev.2009.02.011

374 to 951-kb. The directions of five *PLP1* duplications were further investigated by fiber-FISH analysis, and all showed tandem duplications. The common manifestations of the disease in patients with *PLP1* mutations or duplications in this study were nystagmus in early infancy, dysmyelination revealed by magnetic resonance imaging (MRI), and auditory brain response abnormalities. Although the grades of dysmyelination estimated by MRI findings were well correlated to the clinical phenotypes of the patients, there is no correlation between the size of the duplications and the phenotypic severity.

Keywords: Array-based comparative genomic hybridization (aCGH); Fiber-FISH; Fluorescence *in situ* hybridization (FISH); Pelizaeus–Merzbacher disease (PMD); Proteolipid protein 1 (*PLP1*)

1. Introduction

Pelizaeus–Merzbacher disease (PMD; MIM#312080) is a rare X-linked recessive neurodegenerative disorder characterized by early onset nystagmus and hypotonia later evolving into spastic tetraparesis, dystonia, ataxia, and developmental delay usually beginning in the first year [1–3]. The main cause of PMD is alterations in the proteolipid protein 1 gene (*PLP1*; MIM#300401) on chromosome Xq22.2 [4–6], which encodes 2 proteins, PLP1 and the splicing variant, DM20, both of which are abundantly expressed in oligodendrocytes [3]. PLP1 is thought to play a major role in myelin sheath formation by promoting sheath compaction [7]. Within the heterogeneous group of dysmyelinating disorders, PMD accounts for 6.5% of all cases [8].

It has been proposed that patients with *PLP1*-related inherited dysmyelinating disorders should be clinically divided into 3 subgroups in order of decreasing severity: connatal, classic, and X-linked spastic paraplegia type 2 (SPG2; MIM#312920) [9]. Duplications of *PLP1* can be found in up to 70% of all patients with PMD, indicating that increased *PLP1* dosage is deleterious for normal myelination [10,11]. Point mutations in *PLP1* have been found in 10–25% of PMD cases with the entire clinical spectrum [11], ranging from the most severe connatal form to the least severe SPG2 form, depending on the affected domain of the protein [9]. Although there are characteristic clinical and radiological features of PMD [1,12], molecular and/or cytogenetic analyses are necessary for final diagnosis because *PLP1* is only expressed in the central nervous system and there are no practical biochemical tests available. The first step in genetic testing should be a genomic dosage analysis of *PLP1* because the major genetic aberration is duplication of *PLP1*. For this purpose, various methods have been used, including southern blotting [6], quantitative polymerase chain reaction (PCR) [13], fluorescence *in situ* hybridization (FISH) [14], multiplex ligation-dependent probe amplification (MLPA) [15], and multiplex amplifiable probe hybridization (MAPH) [16]. Recently, microarray-based comparative genome hybridization (aCGH) has emerged as a novel technology that enables detection and determination of the size of the duplicated or deleted genomic intervals [17]. In case of normal dosage of *PLP1*, nucleotide sequences of *PLP1* should be examined [18]. Here, we report our recent studies to develop comprehensive molecular and cytogenetic analyses to diagnose patients with PMD and to understand the pathogenic mechanism of PMD and its correlation between clinical phenotypes.

2. Materials

Fifteen unrelated male patients (age span from 1 year to 20 years old) with congenital dysmyelination were referred to us for genetic diagnosis based on the clinical diagnosis as PMD. Clinical information and radiographic findings by magnetic resonance imaging (MRI) for the patients were obtained from attending doctors. Based on the approval by the ethics committee at the institution, informed consents were obtained from patient's families, and peripheral blood samples were obtained from all patients. Lymphoblast cell lines were established from lymphocytes extracted from peripheral blood samples by immortalization with Epstein-Barr virus. Three of the fifteen patients (P1, P3, P4) had been diagnosed as having *PLP1* duplications by previously performed comparative PCR amplification method (data not shown).

Genomic DNAs of the patients were extracted from peripheral blood samples using the QIAquick DNA Extraction Kit (QIAGEN, Hamburg, Germany). Metaphase or prometaphase chromosomes were prepared from phytohemagglutinin-stimulated peripheral blood lymphocytes or lymphocyte cell lines according to standard techniques.

One extra cell line (S1) that showed duplication of Xp22.31 including steryl-sulfatase precursor gene (*STS*) as determined by aCGH, was derived from a non-PMD mentally retarded patient and used for fiber-FISH analysis as a positive control of *STS* duplication.

Population-based control DNA samples were obtained from 100 healthy Japanese volunteers.

3. Methods

3.1. aCGH analysis

aCGH analysis, using the Human Genome CGH Microarray 105A chip (Agilent Technologies, Santa

Clara, CA), was performed according to the manufacturer's instructions [19]. The data was extracted with Feature Extraction version 9 (Agilent Technologies) and visualized by CGH Analytics version 3.5 (Agilent Technologies). Statistically significant aberrations were determined using the ADM-II algorithm in CGH Analytics version 3.5 (Agilent Technologies).

3.2. Fiber-FISH analysis

Phytohemagglutinin-stimulated lymphocytes or lymphoblasts were harvested using a routine procedure that generates metaphase chromosomes and interphase nuclei. The fiber-FISH slides were prepared as follows: approximately 20 μl of cell suspensions containing metaphase and prometaphase chromosomes were pipetted onto a slide that was then dipped into a 10% sodium dodecyl sulfate (SDS) solution and removed slowly. Bacterial artificial chromosome (BAC) clones were selected from an in-silico library (UCSC Human genome browser, March 2006); RP4-540A13 and RP5-1055C14 mapped to the region surrounding *PLP1*, CTD-2171N231 and RP11-98J1 mapped to the *STS* region of Xp22.31. DNAs from the BAC clones were extracted using GenePrepStar PI-80X (Kurabo, Osaka, Japan), and labeled with digoxigenin-11-dUTP or biotin-16-dUTP (Roche Applied Science, Mannheim, Germany) by nick translation and denatured at 70 °C for 5 min. After hardening process with incubation at 65 °C for 150 min, the chromosome slides were denatured in 70% formamide/2× standard saline citrate (SSC) at 70 °C for 2 min, and then dehydrated at −20 °C in ethanol. The probe-hybridization mixture was applied on the chromosome slides and incubated at 37 °C for more than 16 h. The slides were then washed in 50% formamide/2× SSC at 37 °C for 12 min, 2× SSC at room temperature for 10 min, 1× SSC for 10 min, and 4× SSC for 10 min. And finally, the slides were incubated with 1% bovine serum albumin (BSA), 4× SSC, Fluorescein anti-biotin (Vector, Burlingame, CA, USA) and Anti-digoxigenin-rhodamine, Fab fragments (Roche) at 37 °C for 1 h. Slides were washed 3 times: in 4× SSC for 5 min, in 0.05% Triton-X-100/4× SSC for 5 min with shaking, and finally in 4× SSC for 5 min. The slides were then mounted in antifade solution containing 4′,6-diamino-2-phenylindole (DAPI) stain. Photomicroscopy was performed using a LICA CTR6000 microscope containing a quad filter set with single band excitation filters (Leica Microsystems, Tokyo, Japan).

3.3. PLP1 mutation analysis

The sequence of the patients' 7 coding exons of *PLP1* was determined using the neighboring intronic primers reported by Hobson et al. [20] and a BigDye Terminator Cycle Sequencing kit according to the manufacturer's protocol (Applied Biosystems, Foster City, CA). One hundred control samples were genotyped to verify that the *PLP1* mutation identified in the PMD patients was not found in the general population.

4. Results and discussion

4.1. Genetic diagnosis of PMD

Three distinct genetic mechanisms responsible for PMD have been reported: (1) Loss of PLP1 function caused by null mutations or deletions; (2) gain of toxic function (the PLP1 mutant protein accumulates in the endoplasmic reticulum, triggering increased oligodendrocyte cell death by apoptosis resulting in dysmyelination); (3) overexpression of PLP1 due to genomic duplication [3,7]. As mentioned in Section 2, three (P1, P3, and P4) of the 15 patients had been diagnosed as having *PLP1* duplications by previously performed comparative PCR amplification method, which were re-confirmed by aCGH and fiber-FISH in this study. Subsequently, two (P2 and P5) of the remaining twelve subjects were newly diagnosed as having *PLP1* duplications by aCGH. For the remaining ten patients without genomic duplications, we analyzed the genomic sequence of *PLP1* and identified three missense mutations, one splicing mutation, and one 3-bp deletion (Table 1). Thus, we were unable to determine genetic causes for the phenotype in the remaining five patients, and there is no patient who showed deletion of *PLP1*.

4.2. Detection of genomic duplications of PLP1 by aCGH

aCGH is a revolutionary platform that has been recently adopted in the clinical laboratory. The primary advantage of aCGH is that the array is capable of simultaneously detecting DNA copy changes at multiple loci over the whole genome [21].

In the present study, aCGH analysis identified gains of genomic copy numbers including *PLP1* in five subjects (P1, P2, P3, P4, P5), and the sizes of the chromosomal duplications were 374, 461, 676, 858, and 951-kb, respectively (Table 1 and Fig. 1a). The 461-kb duplication identified in P2 was not detected using standard FISH analysis at another medical facility previously, indicating the advantages of aCGH testing for PMD. There was no genomic copy number aberration in the remaining ten subjects (data not shown). A genomic copy number gain was identified on Xp22.31 with the size of 1.5-Mb in the sample from S1 (Fig. 1b).

4.3. Fiber-FISH analysis

aCGH holds the promise of being the initial diagnostic tool in the identification of visible and submicroscopic

Table 1
Clinical characteristics of the patients with PLP1 duplications or mutations.

	P1	P2	P3	P4	P5	P6	P7	P8	P9	P10
Clinical subtype	Connatal	Classic	Connatal	Connatal	Connatal	Connatal	Connatal	Connatal	Connatal	Connatal
Age at examination	1 year	14 years	20 years	4 months	2 years	2 years	1 year	1 year	4 months	1 year 5 months
Disease onset	1 month	1 day	NA	1 day	1 month	2 months	1 day	1 week	1 month	1 month
Symptoms at onset	Nystagmus	Nystagmus	NA	Nystagmus	Nystagmus Hypotonia	Nystagmus	Asphyxia	Abnormal ABR	Microcephaly*	Nystagmus
Severity score	0	2	0	0	0	0	0	0	0	0
Family history	+	None	NA	None	None	None	None	None	None	None
Age at death				4 years						
Psychomotor development										
Head control	None	7 months	None	None	None	None	None	None	None	None
Sitting	None	4 years	None	None	None	None	None	None	None	None
Walking	None	4 years	None	None	None	None	None	None	None	None
Last evaluation	14 years	14 years	33 years	4 years	2 years	2 years	1 year	4 years	5 months	1 year 5 months
Neurological signs										
Nystagmus	+	+	None	+	+	+	+	+	+	+
Muscular hypotonia	+	None	+	+	+	+ (upper limbs)	+	+	+	+
Pyramidal signs	None	+	+		+	+ (lower limbs)	None	None	None	
Ataxia		+								
Tremor	+									
Seizures				+				+	+	Sensori-neural
deafness										
Other symptoms		Dysarthria		Choreoathetosis			Strider		Microcephaly	
Disease course		Deterioration; now only sitting								
ABR findings	Only I–III waves	Only I–III waves	NA	Only I wave	Only I wave	Only I wave	Only I–III waves	Only I wave	Only I wave	Only I–II waves
MRI findings	Delayed myelination	Incomplete myelination	NA	Hypomyelination	Hypomyelination	Delayed myelination	Delayed myelination	Delayed myelination	Delayed myelination	Hypomyelination
Genotype	Duplication	Duplication	Duplication	Duplication	Duplication	Missense mutation exon 2c.149A> G(p.Tyr50Cys)	Missense mutation exon 3c.247G> A(p.Gly83Arg)	Missense mutation exon 3c.254TA> Cp.Leu85Pro	Splicing mutation intron 3IVS3-1G>C (splicing error)	Nucleotide deletion exon 3c.238_240delTTC (p.Phe80del)
	374-kb	461-kb	676-kb	858-kb	951-kb					

*, His microcephaly is −3.2SD; NA, not available; MRI, magnetic resonance imaging; ABR, auditory brain response.

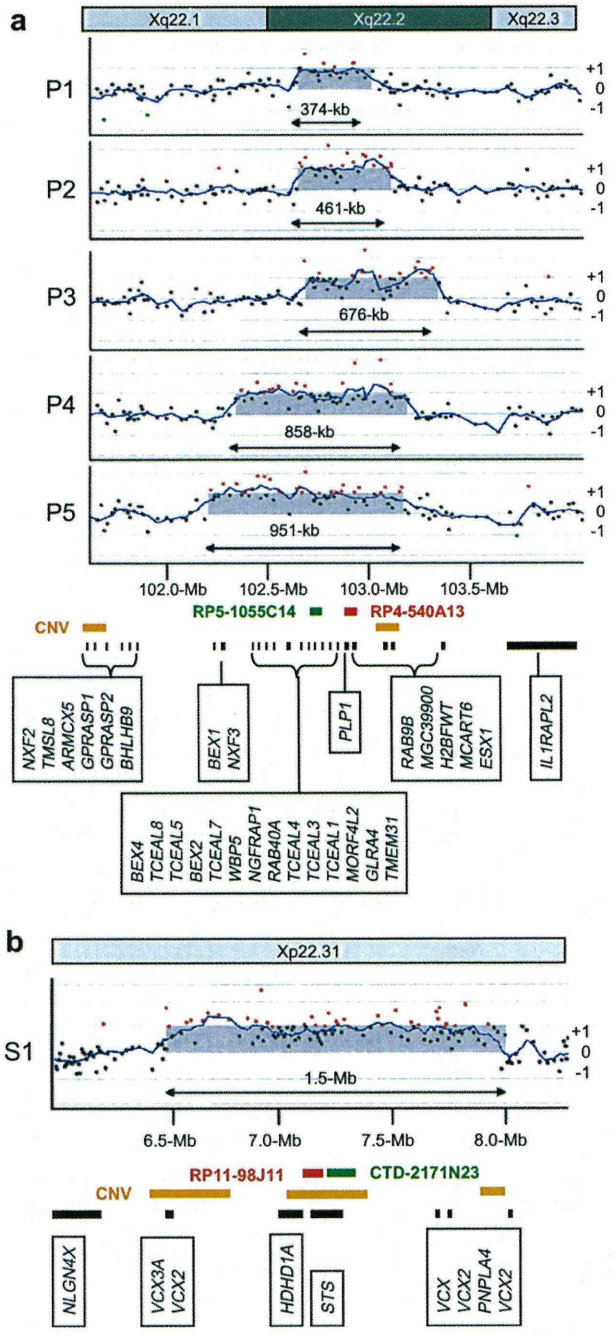

Fig. 1. Results of aCGH. CGH Analytics ver 3.5 (Agilent technologies) visualized genomic copy number aberration on Xq22.2 including *PLP1* (P1, P2, P3, P4, P5) (a) and on Xp22.31 including *STS* (S1) (b). The *X*-axis indicates physical position of chromosome X, and the scales of chromosome bands and physical position were depicted top and bottom, respectively. The *Y*-axis indicates the signal $\log_2$ ratio; positive and negative numbers indicate gain and loss of genomic copy numbers, respectively. The locations of the indicated genes (black rectangles), known copy number variations (CNVs) (orange rectangles), and the two BAC probes used in fiber-FISH analyses with green and red rectangles are shown under the figure depicted on the map according to the scale.

chromosome abnormalities [22], but it does not provide genome position or orientation information. Several cases have been reported in which the duplication is non-contiguous and the additional copy is found in a cytogenetically distinguishable band on the X chromosome (Xq22 and Xq26.3) [23]. Therefore, we should reconfirm the results of aCGH by another method including FISH analysis, especially in case of genetic counseling [23].

We checked the signals by conventional FISH analysis using metaphase, and translocations were denied in all samples (data not shown). Subsequently, two-color fiber-FISH analyses were performed to confirm the directions of the genomic duplications of *PLP1* in the five subjects, and the all duplicated segments were inserted in tandem (Fig. 2). The subjects with the longer duplicated regions (P4 and P5) showed longer intervals between the 2 sets of probe signals, which are consistent with the results of the aCGH analysis (Fig. 1a). The gain of genomic copy number on Xp22.31 in S1 was also analyzed by fiber-FISH, which showed inverted segments (Fig. 2).

Detection and visualization of *PLP1* duplications require specific molecular and cytogenetic technologies. Duplication of chromosomal regions can be determined by FISH analysis as a doublet signal in interphase chromosomes derived from immortalized lymphocyte cell lines [14,24]. However, when the duplicated region is very small and the locations of the duplicated segments are too close to each other, it is difficult to identify signals independently even if we use interphase chromosomes. In such cases, stretched chromatins rather than

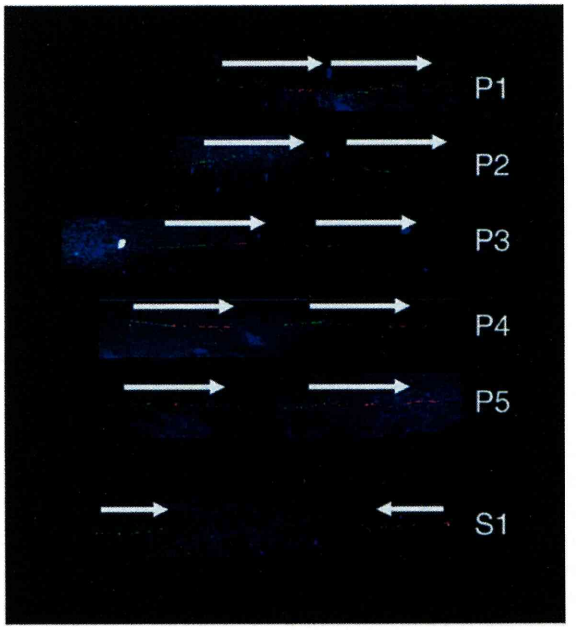

Fig. 2. The results of two-color fiber-FISH analyses. White arrows indicate the direction of duplicated segments.

the conventional interphase or metaphase chromosomes can be used for fiber-FISH analysis [25]. In this technique, two copies of the gene can be visualized as a doublet signal [14].

Interestingly, in PMD patients with *PLP1* duplications, the rearrangement breakpoints for each patient are different, yielding duplicated genomic segments of varying lengths [25–28]. Based on the genomic region around *PLP1*, Woodward et al. suggest that duplicated segments or low copy repeats (LCRs) may promote instability [26]. In this study, the distal ends of the duplicated segments were located in a copy number variation (CNV) region (cnp1417: 102,969,058–103,341,717) [29] in all five subjects, and the proximal ends were differently expanded (Fig. 1a). These findings were similar to the majority of the 11 duplications found by Woodward et al. [26]. Additional studies have shown that *PLP1* duplication events may be stimulated by LCRs or by nonhomologous pairs at both the proximal and distal breakpoints [21]. Despite the variation in size, the duplications encompassing *PLP1* are usually found in tandem [26,30]. All of our subjects with *PLP1* duplications had tandem duplications, as revealed by fiber-FISH analysis (Fig. 2). We also analyzed the region of microduplications of *STS* on Xp22.31, known as the CNV region, by fiver-FISH, which demonstrated that the duplicated segment was inserted in inverted direction (Fig. 2). This indicates that the chromosomal duplication mechanism varies depending on the location.

4.4. PLP1 mutations

To attempt to identify the genomic anomalies responsible for PMD in the remaining ten patients without *PLP1* duplications, we sequenced all the seven exons of *PLP1* and identified nucleotide alterations in five patients (Table 1, Fig. 3). Three of them were missense mutations, i.e. c.149A>G (p.Tyr50Cys) in exon 2, c.247G>A (p.Gly83Arg) in exon 3, and c.254T>C (p.Leu85Pro) in exon 3, in P6, P7, and P8, respectively. One was a splicing mutation, IVS3-1G>C in intron 3, in P9. Another was 3-bp deletion, c.238_240delCTT (p.Phe80del) in exon 3, in P10. Although c.149A>G was previously reported by Hübner et al. [18], the others were novel.

The two missense substitutions, c.247G>A and c.254T>C, are located within the second hydrophobic transmembrane domain. The nucleotide alteration, IVS3-1G>C, is located within the consensus splicing acceptor site. There is a similar known splicing mutation at the same splicing acceptor site, but it was IVS3-1G>T [31]. As PLP1 is expressed only in the central nervous system, we cannot confirm splicing alterations by RT-PCR. However, the mutations in the consensus splicing sites are believed to cause splicing abnormalities. The other novel 3-bp deletion, c.238_240delTTC, in exon 3 will cause in-frame amino acid deletion. All four novel

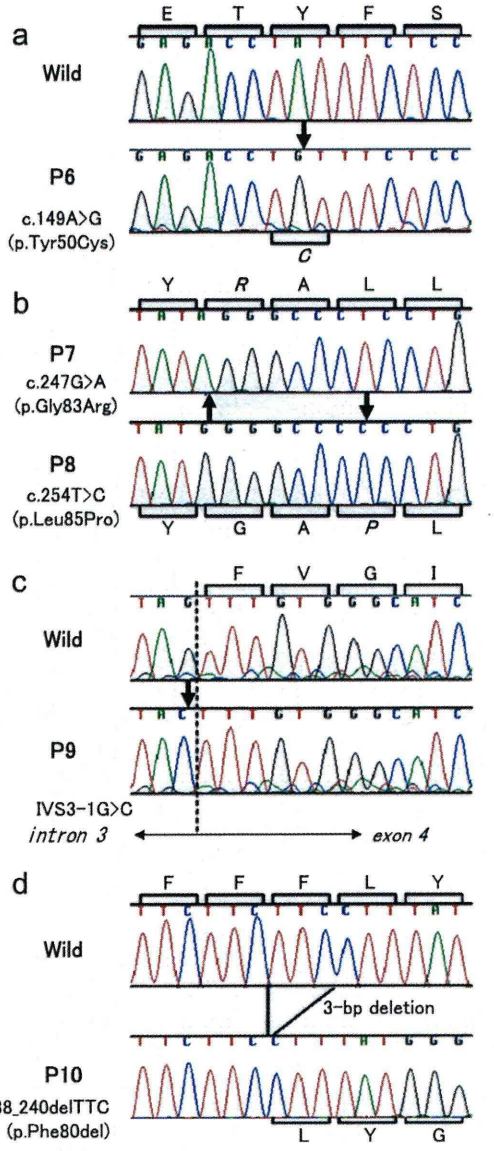

Fig. 3. Partial sequence electrophoregrams of *PLP1* mutations identified in this study. Thick arrows and italic amino acid symbols indicate the positions of mutations and altered amino acids, respectively. The broken line indicates exon–intron boundary (C). wild; sequence of wild type.

mutations were not detected in the 100 control samples, leading us to conclude that these should not be polymorphisms. Because it is well known that the genomic sequence of *PLP1* is highly conserved between species [32], these novel mutations should be pathogenic for patients with PMD. Previously, we reported two pathogenic *PLP1* mutations identified on the patients with the connatal form of PMD, and one of which, jimpy^{msd} mutation, was identical with the mice model [33,34]. Including them, more than 100 *PLP1* mutations have been reported to date (see the GeneTests Web site: http://www.genetests.org). Mutations

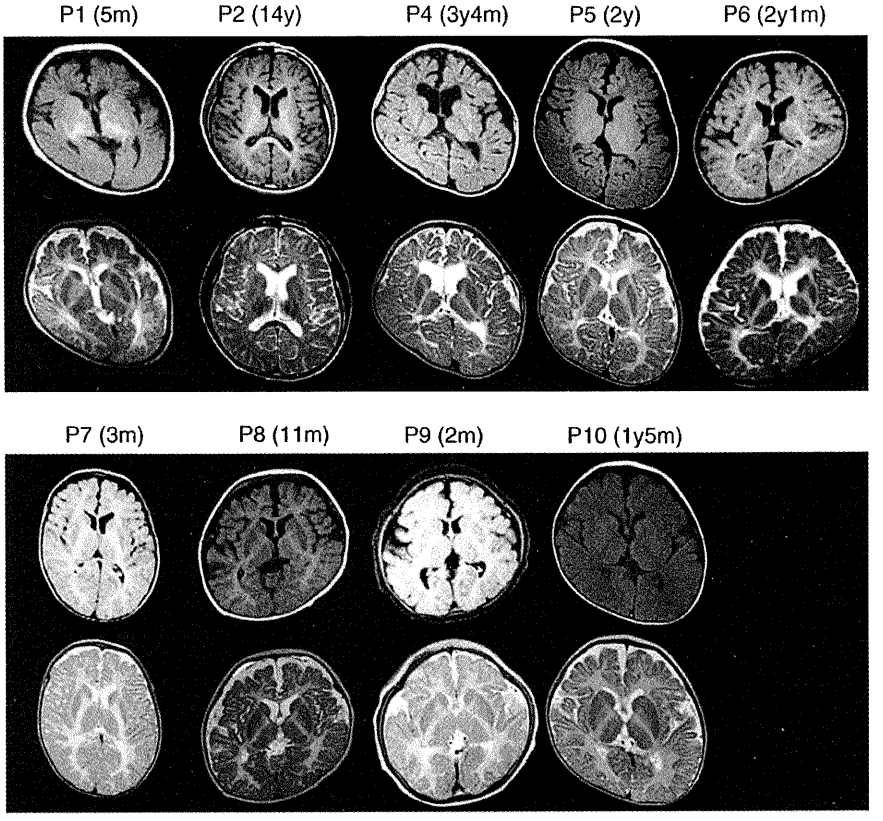

Fig. 4. Brain MRIs of nine patients analyzed in this study. Axial T1- and T2-weighted images are in the top and bottom rows, respectively. Ages at the time of examination are shown in brackets. y; years, m; months.

are distributed throughout all of the *PLP1* coding exons, and each mutation is usually unique to a family [7]. The fact that the majority of *PLP1* missense mutations cause more severe phenotypes than null mutations suggests that the profound dysmyelination resulting from *PLP1* point mutations probably arises not from the absence of functional protein, but rather from a cytotoxic effect of the mutant protein [3].

4.5. Correlation of PLP1 genotypes with PMD phenotypes

The clinical phenotypes of ten subjects who were diagnosed as having *PLP1* duplications (five) or *PLP1* nucleotide alterations (five) are summarized in Table 1. P2 is the only patient with the milder classic form of PMD, and demonstrated the greatest walking ability of all cases in this study. The other subjects were diagnosed with the connatal form of PMD with severe developmental delay. P4 died at age 4, although no details were provided.

Brain MRIs were obtained from nine patients and shown in Fig. 4. All of them showed abnormal intensity in the white matter. Although P2 showed normal high intensity in T1-weighted image (T1), that of the frontal lobe in T2-weighted image (T2) is higher than that of the occipital. This indicated incomplete myelination. P6, P7, P8, and P9 showed high intensity in both T1 and T2, indicating delayed myelination. P1 showed low intensity in T1, and high intensity in T2. As these MRIs were obtained when he was 5 months old, this indicated delayed myelination. P4, P5, and P10 showed low intensity in T1, and high intensity in T2, indicating very severe hypomyelination.

All ten patients having a *PLP1* mutation or duplication showed nystagmus in early infancy, dysmyelination revealed by MRI, and auditory brain response (ABR) abnormalities (Table 1). This triad of presenting symptoms should be the clue to get a clinical diagnosis of PMD. Regarding the radiological findings of the patients, all the provided MRI findings showed dysmyelination with varying degrees (Fig. 4). P4 with the most severe phenotype of PMD showed very low intensity white matter in the T1-weighted imaging, whereas P2 with the mildest form of PMD showed only mildly affected incomplete myelination in T2-weighted imaging. These MRI findings are well-correlated with the clinical severity.

All five patients with nucleotide alterations in *PLP1* displayed the very severe connatal type PMD, whereas P2 whose genome contained a small duplication including *PLP1* showed the milder classical type PMD. These results agree with previous reports showing that the phe-

notypes of patients with genomic duplications are generally milder than those with nucleotide mutations [3]. However, the other four patients with *PLP1* duplications, P1, P3, P4, and P5, displayed the severe connatal form of PMD.

P4 showed a large duplicated region and died when he was 4 years old. On the other hand, P1 contained a very small duplicated segment, similar to P2 in the length, but displayed a very severe phenotype. Thus, it appears that, as suggested by Regis et al., the extent of the duplicated genomic segments does not correlate with clinical severity [35].

According to Lee et al., 65% of patients with *PLP1* duplications have complex rearrangements in nucleotide sequence levels [28]. In this study, we detected *PLP1* duplications by aCGH, and the directions of those duplicated regions were determined by fiber-FISH. However, there is still the possibility that more complicated small rearrangements exist in the duplicated region, particularly in P1. The existence of more complicated rearrangements may explain the reason why there is no correlation between the size of the duplication and the phenotypic severity.

4.6. Differential diagnosis

After genetic evaluation of *PLP1*, the five patients, who did not show any mutations in *PLP1*, were re-evaluated, and one of them was diagnosed as having metachromatic leukodystrophy in the other institution. Another patient showed congenital leukodystrophy with migrating partial seizures in infancy, but no nystagmus and no ABR abnormality, indicating that PMD would be misdiagnosis. Since the other three patients fulfilled the triad described above, the disease-causing mutations might be on the non-coding upstream region of PLP1, or on the other candidate genes for congenital leukodystrophy, including the gap junction protein α12 (GJA12) and others [36,37].

Acknowledgements

This work was supported by the International Research and Educational Institute for Integrated Medical Sciences, Tokyo Women's Medical University, which is supported by the Program for Promoting the Establishment of Strategic Research Centers, Special Coordination Funds for Promoting Science and Technology, Ministry of Education, Culture, Sports, Science and Technology (Japan).

References

[1] Boulloche J, Aicardi J. Pelizaeus–Merzbacher disease: clinical and nosological study. J Child Neurol 1986;1:233–9.
[2] Koeppen AH, Robitaille Y. Pelizaeus–Merzbacher disease. J Neuropathol Exp Neurol 2002;61:747–59.
[3] Inoue K. PLP1-related inherited dysmyelinating disorders: Pelizaeus–Merzbacher disease and spastic paraplegia type 2. Neurogenetics 2005;6:1–16.
[4] Hudson LD, Puckett C, Berndt J, Chan J, Gencic S. Mutation of the proteolipid protein gene PLP in a human X chromosome-linked myelin disorder. Proc Natl Acad Sci USA 1989;86:8128–31.
[5] Gencic S, Abuelo D, Ambler M, Hudson LD. Pelizaeus–Merzbacher disease: an X-linked neurologic disorder of myelin metabolism with a novel mutation in the gene encoding proteolipid protein. Am J Hum Genet 1989;45:435–42.
[6] Ellis D, Malcolm S. Proteolipid protein gene dosage effect in Pelizaeus–Merzbacher disease. Nat Genet 1994;6:333–4.
[7] Garbern JY. Pelizaeus–Merzbacher disease: genetic and cellular pathogenesis. Cell Mol Life Sci 2007;64:50–65.
[8] Heim P, Claussen M, Hoffmann B, Conzelmann E, Gartner J, Harzer K, et al. Leukodystrophy incidence in Germany. Am J Med Genet 1997;71:475–8.
[9] Cailloux F, Gauthier-Barichard F, Mimault C, Isabelle V, Courtois V, Giraud G, et al. Genotype-phenotype correlation in inherited brain myelination defects due to proteolipid protein gene mutations. Clinical European network on brain dysmyelinating disease. Eur J Hum Genet 2000;8:837–45.
[10] Sistermans EA, de Coo RF, De Wijs IJ, Van Oost BA. Duplication of the proteolipid protein gene is the major cause of Pelizaeus–Merzbacher disease. Neurology 1998;50:1749–54.
[11] Mimault C, Giraud G, Courtois V, Cailloux F, Boire JY, Dastugue B, et al. Proteolipoprotein gene analysis in 82 patients with sporadic Pelizaeus–Merzbacher disease: duplications, the major cause of the disease, originate more frequently in male germ cells, but point mutations do not. The clinical European network on brain dysmyelinating disease. Am J Hum Genet 1999;65:360–9.
[12] Caro PA, Marks HG. Magnetic resonance imaging and computed tomography in Pelizaeus–Merzbacher disease. Magn Reson Imaging 1990;8:791–6.
[13] Inoue K, Osaka H, Sugiyama N, Kawanishi C, Onishi H, Nezu A, et al. A duplicated PLP gene causing Pelizaeus–Merzbacher disease detected by comparative multiplex PCR. Am J Hum Genet 1996;59:32–9.
[14] Woodward K, Kendall E, Vetrie D, Malcolm S. Pelizaeus–Merzbacher disease: identification of Xq22 proteolipid-protein duplications and characterization of breakpoints by interphase FISH. Am J Hum Genet 1998;63:207–17.
[15] Wolf NI, Sistermans EA, Cundall M, Hobson GM, Davis-Williams AP, Palmer R, et al. Three or more copies of the proteolipid protein gene PLP1 cause severe Pelizaeus–Merzbacher disease. Brain 2005;128:743–51.
[16] Combes P, Bonnet-Dupeyron MN, Gauthier-Barichard F, Schiffmann R, Bertini E, Rodriguez D, et al. PLP1 and GPM6B intragenic copy number analysis by MAPH in 262 patients with hypomyelinating leukodystrophies: identification of one partial triplication and two partial deletions of PLP1. Neurogenetics 2006;7:31–7.
[17] Lee JA, Cheung SW, Ward PA, Inoue K, Lupski JR. Prenatal diagnosis of PLP1 copy number by array comparative genomic hybridization. Prenat Diagn 2005;25:1188–91.
[18] Hubner CA, Orth U, Senning A, Steglich C, Kohlschutter A, Korinthenberg R, et al. Seventeen novel PLP1 mutations in patients with Pelizaeus–Merzbacher disease. Hum Mutat 2005;25:321–2.
[19] Bartocci A, Striano P, Mancardi MM, Fichera M, Castiglia L, Galesi O, et al. Partial monosomy Xq(Xq23 -> qter) and trisomy 4p(4p15.33 -> pter) in a woman with intractable focal epilepsy, borderline intellectual functioning, and dysmorphic features. Brain Dev 2008;30:425–9.
[20] Hobson GM, Davis AP, Stowell NC, Kolodny EH, Sistermans EA, de Coo IF, et al. Mutations in noncoding regions of the proteolipid protein gene in Pelizaeus–Merzbacher disease. Neurology 2000;55:1089–96.

[21] Bejjani BA, Shaffer LG. Application of array-based comparative genomic hybridization to clinical diagnostics. J Mol Diagn 2006;8:528–33.
[22] Shaffer LG, Bejjani BA. Medical applications of array CGH and the transformation of clinical cytogenetics. Cytogenet Genome Res 2006;115:303–9.
[23] Woodward K, Cundall M, Palmer R, Surtees R, Winter RM, Malcolm S. Complex chromosomal rearrangement and associated counseling issues in a family with Pelizaeus–Merzbacher disease. Am J Med Genet A 2003;118A:15–24.
[24] Inoue K, Kanai M, Tanabe Y, Kubota T, Kashork CD, Wakui K, et al. Prenatal interphase FISH diagnosis of PLP1 duplication associated with Pelizaeus–Merzbacher disease. Prenat Diagn 2001;21:1133–6.
[25] Inoue K, Osaka H, Imaizumi K, Nezu A, Takanashi J, Arii J, et al. Proteolipid protein gene duplications causing Pelizaeus–Merzbacher disease: molecular mechanism and phenotypic manifestations. Ann Neurol 1999;45:624–32.
[26] Woodward KJ, Cundall M, Sperle K, Sistermans EA, Ross M, Howell G, et al. Heterogeneous duplications in patients with Pelizaeus–Merzbacher disease suggest a mechanism of coupled homologous and nonhomologous recombination. Am J Hum Genet 2005;77:966–87.
[27] Lee JA, Inoue K, Cheung SW, Shaw CA, Stankiewicz P, Lupski JR. Role of genomic architecture in PLP1 duplication causing Pelizaeus–Merzbacher disease. Hum Mol Genet 2006;15:2250–65.
[28] Lee JA, Carvalho CM, Lupski JR. A DNA replication mechanism for generating nonrecurrent rearrangements associated with genomic disorders. Cell 2007;131:1235–47.
[29] Redon R, Ishikawa S, Fitch KR, Feuk L, Perry GH, Andrews TD, et al. Global variation in copy number in the human genome. Nature 2006;444:444–54.
[30] Inoue K. Pelizaeus–Merzbacher disease and spastic paraplegia type 2. In: Lupski JR, Stankiewicz P, editors. Genomic disorders. Totowa, NJ: Humana press; 2006. p. 263–9.
[31] Strautnieks S, Malcolm S. A G to T mutation at a splice site in a case of Pelizaeus–Merzbacher disease. Hum Mol Genet 1993;2:2191–2.
[32] Diehl HJ, Schaich M, Budzinski RM, Stoffel W. Individual exons encode the integral membrane domains of human myelin proteolipid protein. Proc Natl Acad Sci USA 1986;83:9807–11.
[33] Yamamoto T, Nanba E, Zhang H, Sasaki M, Komaki H, Takeshita K. Jimpy(msd) mouse mutation and connatal Pelizaeus–Merzbacher disease. Am J Med Genet 1998;75:439–40.
[34] Yamamoto T, Nanba E. A novel mutation (A246T) in exon 6 of the proteolipid protein gene associated with connatal Pelizaeus–Merzbacher disease. Hum Mutat 1999;14:182.
[35] Regis S, Biancheri R, Bertini E, Burlina A, Lualdi S, Bianco MG, et al. Genotype-phenotype correlation in five Pelizaeus–Merzbacher disease patients with PLP1 gene duplications. Clin Genet 2008;73:279–87.
[36] Uhlenberg B, Schuelke M, Ruschendorf F, Ruf N, Kaindl AM, Henneke M, et al. Mutations in the gene encoding gap junction protein alpha 12 (connexin 46.6) cause Pelizaeus–Merzbacher-like disease. Am J Hum Genet 2004;75:251–60.
[37] Henneke M, Combes P, Diekmann S, Bertini E, Brockmann K, Burlina AP, et al. GJA12 mutations are a rare cause of Pelizaeus–Merzbacher-like disease. Neurology 2008;70:748–54.

LETTERS

A case of sporadic adult Alexander disease presenting with acute onset, remission and relapse

INTRODUCTION

Adult Alexander disease is a rare leucodystrophy with severe atrophy of the lower brainstem and upper cervical cord.[1] The pathological character is the presence of Rosenthal fibres that contain aggregates of intermediate protein, GFAP, associated with mutations in *GFAP* gene.[2] Because pathogenesis is degenerative, the most typical clinical course is slowly progressive; the intermittent course has not been sufficiently described so far.[2] We show a case of genetically confirmed adult Alexander's disease with acute exaggeration and remission, and relapse.

CASE REPORT

A 33-year-old woman had been well until she suddenly fell down and lost consciousness in 2002. She had left-sided paresis and dysarthria, and was admitted to a hospital. Her medical history was unremarkable except for mild diabetes mellitus. There was no family history of neurological diseases or consanguineous marriage. Her father died of heart disease (in his 40s), her mother died of diabetes mellitus and angina pectoris (in her 50s), and her two daughters were healthy. Brain MRI showed atrophy of the upper cervical cord and T2-hyperintensity in the bilateral periventricular areas and the medulla. The patient was treated for acute ischaemic stroke with medical therapy and rehabilitation (figure 1A). She gradually improved, with the ability to walk with an aid 6 months after the onset and was discharged home 1 year after the onset with left-sided weakness and slight dysarthria. There was no exacerbation or improvement of weakness and dysarthria after this episode until the age of 39, when she developed high-grade fever and respiratory failure followed by limb weakness. These symptoms worsened over 1 week, and she was admitted to another hospital and treated for pneumonia, which required mechanical ventilation, tracheostomy and percutaneous endoscopic gastrostomy (PEG). Although pneumonia improved and she was weaned from mechanical ventilation, the patient was still bed-ridden with tetraparesis, severe dysarthria and dysphagia. She was referred to our hospital 5 months later for further neurological evaluation.

The patient was normotensive, alert and well oriented, which was evident by her response with preserved facial expressions. Optic fundi and nerves were normal. Her

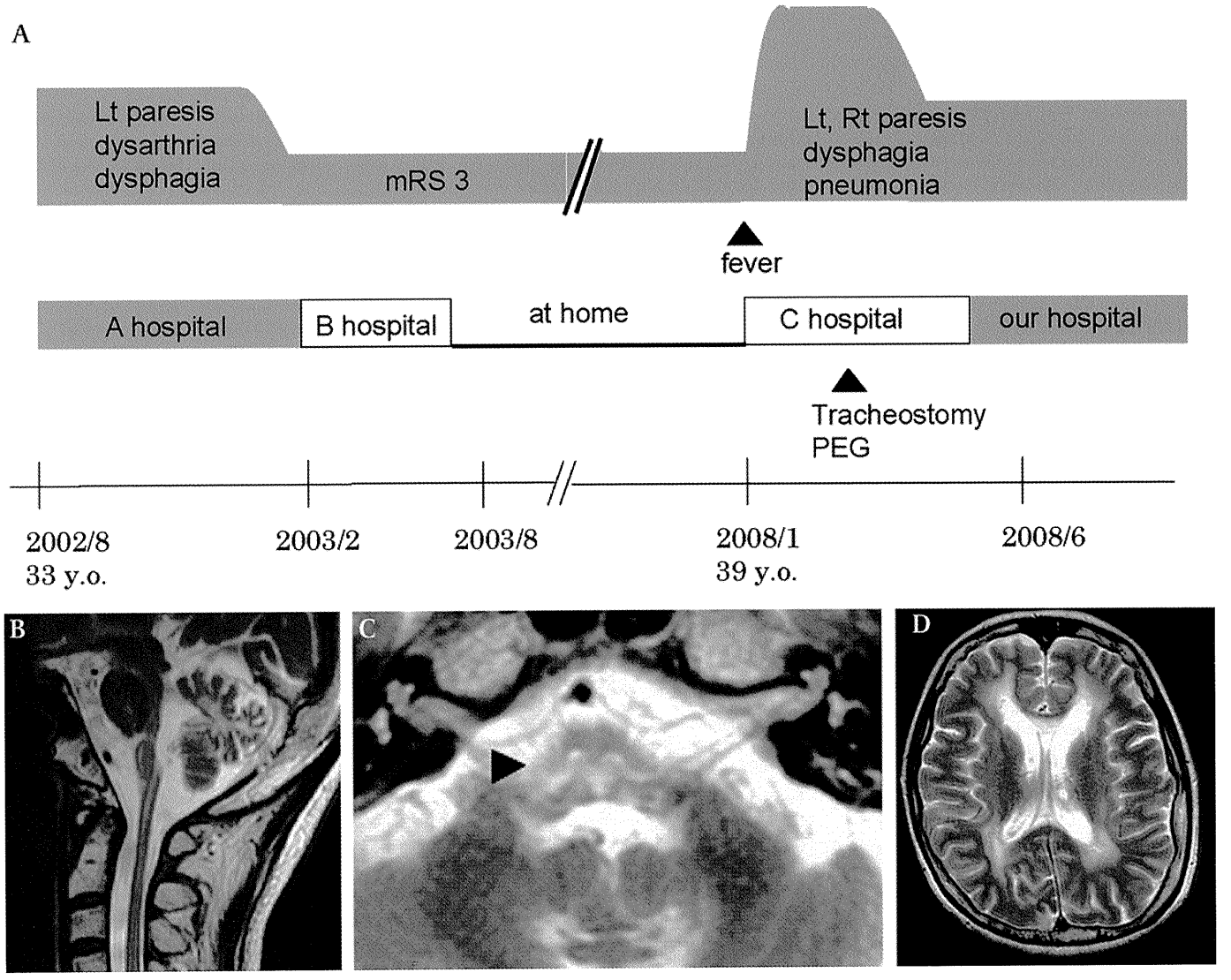

Figure 1 (A) Clinical course. mRS, modified Rankin Scale; PEG, percutaneous endoscopic gastrostomy. (B) Sagittal and (C), (D) axial T2 weighted MRI of brain. Severe atrophy extends from the medulla to the upper cervical cord (B). There is hyperintensity in the medulla (C arrowhead) and the periventricular area (D).